

# **SOPTX: A High-Performance Multi-Backend Framework for Topology Optimization**

Liang He<sup>1</sup>, Long Chen<sup>2</sup>, Xuehai Huang<sup>3,\*</sup>, Huayi Wei<sup>1</sup>

<sup>1</sup> *School of Mathematics and Computational Science, Xiangtan University; National Center of Applied Mathematics in Hunan, Hunan Key Laboratory for Computation and Simulation in Science and Engineering Xiangtan 411105, China*

<sup>2</sup> *Department of Mathematics, University of California at Irvine, Irvine, CA 92697, USA*

<sup>3</sup> *School of Mathematics, Shanghai University of Finance and Economics, Shanghai 200433, China*

---

\*Corresponding author. *Email addresses:* cbtnxs@smail.xtu.edu.cn (C. Chen), chenlong@math.uci.edu (L. Chen), huang.xuehai@sufe.edu.cn (X. Huang), weihuayi@xtu.edu.cn (H. Wei)

**Abstract.** In recent years, topology optimization (TO) has gained widespread attention in both industry and academia as an ideal structural design method. However, its application has high barriers to entry due to the deep expertise and extensive development work typically required. Traditional numerical methods for TO are tightly coupled with computational mechanics methods such as finite element analysis (FEA), making the algorithms intrusive and requiring comprehensive understanding of the entire system. This paper presents SOPTX, a TO package based on FEALPy, which implements a modular architecture that decouples analysis from optimization, supports multiple computational backends (NumPy/PyTorch/JAX), and achieves a non-intrusive design paradigm.

The main innovations of SOPTX include: (1) A cross-platform, multi-backend support system compatible with various computational backends such as NumPy, PyTorch, and JAX, enabling efficient algorithm execution on CPUs and flexible acceleration using GPUs, as well as efficient sensitivity computation for objective and constraint functions via automatic differentiation (AD); (2) A fast matrix assembly technique, overcoming the performance bottleneck of traditional numerical integration methods and significantly enhancing computational efficiency; (3) A modular framework designed to support TO problems for arbitrary dimensions and meshes, complemented by a rich library of composable components, including diverse filters and optimization methods, enabling users to flexibly configure and extend optimization workflows according to specific needs.

Taking the density-based method as an example, this paper elaborates the architecture, computational workflow, and usage of SOPTX through the classical compliance minimization problem with volume constraints. Numerical examples demonstrate that SOPTX significantly outperforms existing open-source packages in terms of computational efficiency and memory usage, especially exhibiting superior performance in large-scale problems. The modular design of the software not only enhances the flexibility and extensibility of the code but also provides opportunities for exploring novel TO problems, offering robust support for education, research, and engineering applications in TO.

**AMS subject classifications:** 65N30, 35Q60

**Key words:** Implementation of Finite Elements, Nodal Finite Elements,  $H(\text{curl})$ -Conforming,  $H(\text{div})$ -Conforming

---

## 1 Introduction

Topology optimization (TO) is an essential class of structural optimization techniques aimed at improving structural performance by optimizing material distribution within a design domain. In fields such as aerospace, automotive, and civil engineering, TO addresses critical design challenges through efficient material utilization and mechanical performance optimization. Among various approaches, density-based methods are particularly popular due to their intuitiveness and practicality. In these methods, the distribution of material and void within the design domain is optimized, and the relative density of each finite element is treated as a design variable. The most widely adopted density-based method is the Solid Isotropic Material with Penalization (SIMP) approach. This approach promotes binary (0–1) solutions by penalizing intermediate densities,

and due to its simplicity and seamless integration with finite element analysis (FEA), it has been extensively employed since its introduction by [9].

However, TO problems inherently involve large-scale computations. This is due to the tight coupling between structural analysis and element-level optimization of design variables: at each iteration, it is necessary not only to solve boundary value problems to obtain structural responses but also to calculate derivatives of the objective and constraint functions with respect to design variables, supporting gradient-based optimization algorithms. For large-scale problems, this implies solving large linear systems and performing sensitivity analysis at every iteration, placing significant demands on computing resources and performance. Therefore, improving computational efficiency and scalability while ensuring accuracy has become a major challenge in TO research and applications.

To lower the entry barrier and promote widespread adoption of TO, researchers have published numerous educational studies and literature. A pioneering example is the 99-line MATLAB code by [32], which demonstrated the fundamentals of a two-dimensional SIMP algorithm in a concise and self-contained manner, profoundly impacting both TO education and research. Subsequently, improved versions of this educational code emerged continuously, including the more efficient 88-line version proposed by [6] and the extended 3D implementation by [27]. These educational codes convey practical knowledge of TO in the simplest possible form and provide self-contained examples of basic numerical algorithms.

Meanwhile, efforts have also been made to leverage the advantages of open-source software development for addressing TO problems. For example, [19] proposed a modular TO approach based on OpenMDAO [24], an open-source multidisciplinary design optimization framework. They decomposed the TO problem into multiple components, where users provide forward computations and analytic partial derivatives, while OpenMDAO automatically assembles and computes total derivatives, enhancing code flexibility and extensibility. Subsequently, [26] developed a parallel-enabled TO implementation based on the open-source finite element software FEniCS [4], demonstrating its potential for handling large-scale problems. More recently, [23] advanced this direction by introducing a concise and efficient TO implementation in just 51 lines of code. Their work utilized FEniCS for modeling and FEA, Dolfin Adjoint for automatic sensitivity analysis, and Interior Point OPTimizer for optimization, greatly simplifying the implementation process. These projects provided standardized interfaces enabling convenient integration with existing FEA tools, thereby lowering implementation complexity. However, despite improvements in modularity achieved by these open-source software packages, challenges in terms of functionality extension and flexibility remain when dealing with complex engineering applications.

To accelerate the development of TO, automating sensitivity analysis has become a critical step. This involves automatically computing derivatives of objectives, constraints, material models, projections, filters, and other components with respect to the design variables. Currently, the common practice involves manually calculating sensitivities, which, despite not being theoretically complex, can be tedious and error-prone, often becoming a bottleneck in the development of new TO modules and exploratory research. Automatic differentiation (AD) provides an efficient and accurate approach for evaluating derivatives of numerical functions [25]. By decomposing complex functions into a series of elementary operations (such as addition and multiplication),

AD accurately computes derivatives of arbitrary differentiable functions. In TO, the Jacobian matrices represent sensitivities of objective functions and constraints with respect to design variables, and software can automate this process, relieving developers from manually deriving and implementing sensitivity calculations. With its capability of easily obtaining accurate derivative information, AD offers significant advantages in design optimization, particularly for highly non-linear problems.

In recent years, the use of AD in TO has gradually increased. For instance, [30] employed the AD tools CoDiPack and Tapenade to achieve automatic sensitivity analysis in unsteady flow TO, significantly enhancing computational efficiency. [14] leveraged JAX [10], a high-performance Python library, to implement AD within density-based TO, efficiently solving classical topology optimization problems such as compliance minimization.

Although the programs described above—including early educational codes, open-source software implementations, and initial frameworks incorporating AD—have significantly promoted the adoption and development of TO methods, they typically employ a procedural programming paradigm. This approach divides the numerical computation process into multiple interdependent subroutines, leading to a tightly coupled relationship between analysis modules (e.g., FEA) and optimization modules. Such tightly coupled architectures limit code extensibility and reusability: on one hand, the strong interdependencies between subroutines mean that even adding a new objective function or constraint often requires invasive modifications across multiple modules, increasing development time and potentially introducing new errors; on the other hand, this coupled architectural pattern makes it challenging to integrate topology optimization programs as standalone modules within multidisciplinary design optimization (MDO) frameworks or system-level engineering processes. For instance, in aerospace applications, TO modules need seamless integration with other disciplines (such as fluid mechanics or thermodynamics), yet tightly coupled architectures typically result in complicated and inefficient integration procedures, hindering the application of TO in more complex scenarios. Consequently, designing an architecture that decouples analysis from optimization, thereby enhancing extensibility and reusability without sacrificing algorithmic accuracy, has become an important challenge that urgently needs addressing in the TO community.

## 2 Preliminaries

In this section, we provide essential foundations for our study. We introduce multi-indices, simplicial lattices, and interpolation points. We explain sub-simplices and their relations. Furthermore, we introduce the dictionary ordering of simplicial lattices and the concept of bubble polynomials.

### 2.1 Simplicial lattice

A multi-index of length  $n+1$  is an array of non-negative integers:

$$\alpha = (\alpha_0, \alpha_1, \dots, \alpha_n), \quad \alpha_i \in \mathbb{N}, i = 0, \dots, n.$$

The degree or sum of the multi-index is  $|\alpha| = \sum_{i=0}^n \alpha_i$  and factorial is  $\alpha! = \prod_{i=0}^n (\alpha_i!)$ . The set of all multi-indices of length  $n+1$  and degree  $k$  will be called a simplicial lattice and denoted by  $\mathbb{T}_k^n$ , i.e.,

$$\mathbb{T}_k^n = \{\alpha \in \mathbb{N}^{n+1} : |\alpha| = k\}.$$

The elements in  $\mathbb{T}_k^n$  can be linearly indexed by the dictionary ordering  $R_n$ :

$$R_n(\alpha) = \sum_{i=1}^n \binom{\alpha_i + \alpha_{i+1} + \dots + \alpha_n + n - i}{n + 1 - i}.$$

For example, for an element  $\alpha$  in  $\mathbb{T}_k^2$ , the index is given by the mapping:

$$R_2(\alpha) = \frac{(\alpha_1 + \alpha_2)(\alpha_1 + \alpha_2 + 1)}{2} + \alpha_2.$$

Notice that  $\alpha_0$  is not used in the calculation of  $R_n(\alpha)$ .

## 2.2 Interpolation points

Let  $x_0, x_1, \dots, x_n$  be  $n+1$  points in  $\mathbb{R}^n$  and

$$T = \text{Convex}(x_0, x_1, \dots, x_n) = \left\{ \sum_{i=0}^n \lambda_i x_i : 0 \leq \lambda_i \leq 1, \sum_{i=0}^n \lambda_i = 1 \right\},$$

be an  $n$ -simplex, where  $\lambda = (\lambda_0, \dots, \lambda_n)$  is called the barycentric coordinate. We can have a geometric embedding of the algebraic set  $\mathbb{T}_k^n$  as follows:

$$\mathcal{X}_T = \left\{ x_\alpha = \frac{1}{k} \sum_{i=0}^n \alpha_i x_i : \alpha \in \mathbb{T}_k^n \right\},$$

which is called the set of interpolation points with degree  $k$  on  $T$ ; see Fig.1 for  $k=4$  and  $n=2$ . In literature [29], it is called the  $k$ -th order principal lattice of  $n$ -simplex  $T$ . Given  $\alpha \in \mathbb{T}_k^n$ , the barycentric coordinate of  $\alpha$  is given by

$$\lambda(\alpha) = (\alpha_0, \alpha_1, \dots, \alpha_n) / k.$$

The ordering of  $\mathcal{X}_T$  is also given by  $R_n(\alpha)$ . Note that the indexing map  $R_n(\alpha)$  is only a local ordering of the interpolation points on one  $n$ -simplex. In Section 6, we will discuss the global indexing of all interpolation points on the triangulation composed of simplexes.

By this geometric embedding, we can apply operators to the geometric simplex  $T$ . For example,  $\mathcal{X}_{\hat{T}}$  denotes the set of interpolation points in the interior of  $T$  and  $\mathcal{X}_{\partial T}$  is the set of interpolation points on the boundary of  $T$ .

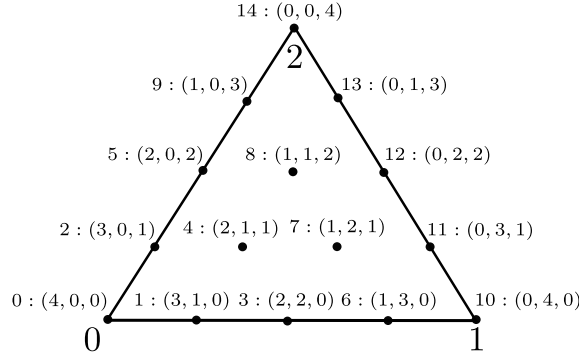


Figure 1: The interpolation points of  $\mathbb{T}_4^2$  and their linear indices and multi-indices.

### 2.3 Sub-simplexes and sub-simplicial lattices

Following [8], let  $\Delta(T)$  denote all the subsimplices of  $T$ , while  $\Delta_\ell(T)$  denotes the set of subsimplices of dimension  $\ell$  for  $\ell = 0, \dots, n$ . The capital letter  $F$  is reserved for an  $(n-1)$ -dimensional face of  $T$  and  $F_i \in \Delta_{n-1}(T)$  denotes the face opposite to  $x_i$  for  $i = 0, 1, \dots, n$ .

For a sub-simplex  $f \in \Delta_\ell(T)$ , following [17], we will overload the notation  $f$  for both the geometric simplex and the algebraic set of indices. Namely  $f = \{f(0), \dots, f(\ell)\} \subseteq \{0, 1, \dots, n\}$  and

$$f = \text{Convex}(x_{f(0)}, \dots, x_{f(\ell)}) \in \Delta_\ell(T)$$

is the  $\ell$ -dimensional simplex spanned by the vertices  $x_{f(0)}, \dots, x_{f(\ell)}$ .

If  $f \in \Delta_\ell(T)$ , then  $f^* \in \Delta_{n-\ell-1}(T)$  denotes the sub-simplex of  $T$  opposite to  $f$ . When treating  $f$  as a subset of  $\{0, 1, \dots, n\}$ ,  $f^* \subseteq \{0, 1, \dots, n\}$  so that  $f \cup f^* = \{0, 1, \dots, n\}$ , i.e.,  $f^*$  is the complement of set  $f$ . Geometrically,

$$f^* = \text{Convex}(x_{f^*(1)}, \dots, x_{f^*(n-\ell)}) \in \Delta_{n-\ell-1}(T)$$

is the  $(n-\ell-1)$ -dimensional simplex spanned by vertices not contained in  $f$ .

Given a sub-simplex  $f \in \Delta_\ell(T)$ , through the geometric embedding  $f \hookrightarrow T$ , we define the prolongation/extension operator  $E: \mathbb{T}_k^\ell \rightarrow \mathbb{T}_k^n$  as follows:

$$E(\alpha)_{f(i)} = \alpha_i, i = 0, \dots, \ell, \quad \text{and} \quad E(\alpha)_j = 0, j \notin f. \quad (2.1)$$

Take  $f = \{1, 3, 4\}$  for example, then the extension  $E(\alpha) = (0, \alpha_0, 0, \alpha_1, \alpha_2, \dots, 0)$  for  $\alpha = (\alpha_0, \alpha_1, \alpha_2) \in \mathbb{T}_k^\ell(f)$ . With a slight abuse of notation, for a node  $\alpha_f \in \mathbb{T}_k^\ell(f)$ , we still use the same notation  $\alpha_f \in \mathbb{T}_k^n(T)$  to denote such extension. The geometric embedding  $x_{E(\alpha)} \in f$  which justifies the notation  $\mathbb{T}_k^\ell(f)$  and its geometric embedding will be denoted by  $\mathcal{X}_f$ , which consists of interpolation points on  $f$ .  $\mathbb{T}_k^\ell(\overset{\circ}{f})$  is the set of lattice points whose geometric embedding is in the interior of  $f$ , i.e.,  $\mathcal{X}_{\overset{\circ}{f}}$ .

The Bernstein representation of polynomial of degree  $k$  on a simplex  $T$  is

$$\mathbb{P}_k(T) := \text{span}\{\lambda^\alpha = \lambda_0^{\alpha_0} \lambda_1^{\alpha_1} \dots \lambda_n^{\alpha_n}, \alpha \in \mathbb{T}_k^n\}.$$

The bubble polynomial of  $f$  is a polynomial of degree  $\ell+1$ :

$$b_f := \lambda_f = \lambda_{f(0)} \lambda_{f(1)} \dots \lambda_{f(\ell)} \in \mathbb{P}_{\ell+1}(f).$$

## 2.4 Triangulation

Let  $\Omega$  be a polyhedral domain in  $\mathbb{R}^n$ ,  $n \geq 1$ . A geometric triangulation  $\mathcal{T}_h$  of  $\Omega$  is a set of  $n$ -simplices such that

$$\cup_{T \in \mathcal{T}_h} T = \Omega, \quad \overset{\circ}{T}_i \cap \overset{\circ}{T}_j = \emptyset, \quad \forall T_i, T_j \in \mathcal{T}_h, T_i \neq T_j.$$

The subscript  $h$  denotes the diameter of each element and can be understood as a piecewise constant function on  $\mathcal{T}_h$ . A triangulation is conforming if the intersection of two simplexes are common lower dimensional sub-simplex. We shall restrict to conforming triangulations in this paper.

The interpolation points on a conforming triangulation  $\mathcal{T}_h$  is

$$\mathcal{X} = \bigcup_{T \in \mathcal{T}_h} \mathcal{X}_T. \quad (2.2)$$

Note that a lot of duplications exist in (2.2). A direct sum of the interpolation set is given by

$$\mathcal{X} = \bigoplus_{\ell=0}^n \bigoplus_{f \in \Delta_\ell(\mathcal{T}_h)} \mathcal{X}_f, \quad (2.3)$$

where  $\Delta_\ell(\mathcal{T}_h)$  denotes the set of  $\ell$ -dimensional subsimplices of  $\mathcal{T}_h$ . In implementation, computation of local matrices on each simplex is based on (2.2) while to assemble a matrix equation, (2.3) should be used. As Lagrange element is globally continuous, the indexing of interpolation points on vertices, edges, faces should be unique and a mapping from the local index to the global index is needed. The index mapping from (2.2) to (2.3) will be discussed in Section 6.

## 3 Geometric Decompositions of Lagrange Elements

In this section, we present a geometric decomposition for Lagrange finite elements on  $n$ -dimensional simplices. We introduce the concept of Lagrange interpolation basis functions, where function values at interpolation points serve as degrees of freedom.

### 3.1 Geometric decomposition

For the polynomial space  $\mathbb{P}_k(T)$  with  $k \geq 1$  on an  $n$ -dimensional simplex  $T$ , we have the following geometric decomposition of Lagrange element [8, (2.6)] and a proof can be found in [16]. The integral at a vertex is understood as the function value at that vertex and  $\mathbb{P}_k(\mathbf{x}) = \mathbb{R}$ .

**Theorem 3.1** (Geometric decomposition of Lagrange element). *For the polynomial space  $\mathbb{P}_k(T)$  with  $k \geq 1$  on an  $n$ -dimensional simplex  $T$ , we have the following decomposition*

$$\mathbb{P}_k(T) = \bigoplus_{\ell=0}^n \bigoplus_{f \in \Delta_\ell(T)} b_f \mathbb{P}_{k-(\ell+1)}(f). \quad (3.1)$$

The function  $u \in \mathbb{P}_k(T)$  is uniquely determined by DoFs

$$\int_f u p \, ds, \quad p \in \mathbb{P}_{k-(\ell+1)}(f), f \in \Delta_\ell(T), \ell = 0, 1, \dots, n. \quad (3.2)$$

Introduce the bubble polynomial space of degree  $k$  on a sub-simplex  $f$  as

$$\mathbb{B}_k(f) := b_f \mathbb{P}_{k-(\ell+1)}(f), \quad f \in \Delta_\ell(T), 1 \leq \ell \leq n.$$

It is called a bubble space as

$$\text{tr}^{\text{grad}} u := u|_{\partial f} = 0, \quad u \in \mathbb{B}_k(f).$$

Then we can write (3.1) as

$$\mathbb{P}_k(T) = \mathbb{P}_1(T) \oplus \bigoplus_{\ell=1}^n \bigoplus_{f \in \Delta_\ell(T)} \mathbb{B}_k(f). \quad (3.3)$$

That is a polynomial of degree  $k$  can be decomposed into a linear polynomial plus bubbles on edges, faces, and all sub-simplices.

Based on a conforming triangulation  $\mathcal{T}_h$ , the  $k$ -th order Lagrange finite element space  $V_k^L(\mathcal{T}_h)$  is defined as

$$V_k^L(\mathcal{T}_h) = \{v \in C(\Omega) : v|_T \in \mathbb{P}_k(T), T \in \mathcal{T}_h, \text{ and DoFs (3.2) are single valued}\},$$

and will have a geometric decomposition

$$V_k^L(\mathcal{T}_h) = V_1^L(\mathcal{T}_h) \oplus \bigoplus_{\ell=1}^n \bigoplus_{f \in \Delta_\ell(\mathcal{T}_h)} \mathbb{B}_k(f). \quad (3.4)$$

Here we extend the polynomial on  $f$  to each element  $T$  containing  $f$  by the Bernstein form and extension of multi-index; see  $E(\alpha)$  defined in (2.1). Consequently the dimension of  $V_k^L$  is

$$V_k^L(\mathcal{T}_h) = \sum_{\ell=0}^n |\Delta_\ell(\mathcal{T}_h)| \binom{k-1}{\ell},$$

where  $|\Delta_\ell(\mathcal{T}_h)|$  is the cardinality of number of  $\Delta_\ell(\mathcal{T}_h)$ , i.e., the number of  $\ell$ -dimensional simplices in  $\mathcal{T}_h$ . We understand  $\binom{k-1}{\ell} = 0$  if  $\ell > k-1$ . That is the degree of the polynomial dictates the dimension of the sub-simplex in the geometric decompositions (3.1) and (3.4).

The geometric decomposition (3.1) can be naturally extended to vector Lagrange elements. For  $k \geq 1$ , define

$$\mathbb{B}_k^n(f) := b_f \mathbb{P}_{k-(\ell+1)}(f) \otimes \mathbb{R}^n.$$

Clearly we have

$$\mathbb{P}_k^n(T) = \mathbb{P}_1^n(T) \oplus \bigoplus_{\ell=1}^n \bigoplus_{f \in \Delta_\ell(T)} \mathbb{B}_k^n(f). \quad (3.5)$$

For an  $f \in \Delta_\ell(T)$ , we choose a  $t-n$  coordinate  $\{\mathbf{t}_i^f, \mathbf{n}_j^f, i=1, \dots, \ell, j=1, \dots, n-\ell\}$  so that

- $\mathcal{T}^f := \text{span}\{\mathbf{t}_1^f, \dots, \mathbf{t}_\ell^f\}$ , is the tangential plane of  $f$ ;
- $\mathcal{N}^f := \text{span}\{\mathbf{n}_1^f, \dots, \mathbf{n}_{n-\ell}^f\}$  is the normal plane of  $f$ .



When  $\ell = 0$ , i.e., for vertices, no tangential component, and for  $\ell = n$ , no normal component. We abbreviate  $\mathbf{n}_1^F$  as  $\mathbf{n}_F$  for  $F \in \Delta_{n-1}(T)$ , and  $\mathbf{t}_1^e$  as  $\mathbf{t}_e$  for  $e \in \Delta_1(T)$ . We have the trivial decompositions

$$\mathbb{R}^n = \mathcal{T}^f \oplus \mathcal{N}^f, \quad \mathbb{B}_k^n(f) = \left[ \mathbb{B}_k(f) \otimes \mathcal{T}^f \right] \oplus \left[ \mathbb{B}_k(f) \otimes \mathcal{N}^f \right]. \quad (3.6)$$

Restricted to an  $\ell$ -dimensional sub-simplex  $f \in \Delta_\ell(T)$ , define

$$\mathbb{B}_k^\ell(f) := \mathbb{B}_k(f) \otimes \mathcal{T}^f,$$

which is a space of  $\ell$ -dimensional vectors on the tangential space  $\mathcal{T}^f$  with vanishing trace  $\text{tr}^{\text{grad}}$  on  $\partial f$ .

When move to a triangulation  $\mathcal{T}_h$ , we shall call a basis of  $\mathcal{T}^f$  or  $\mathcal{N}^f$  is global if it depends only on  $f$  not the element  $T$  containing  $f$ . Otherwise it is called local and may vary in different elements.

### 3.2 Lagrange interpolation basis functions

Previously DoFs (3.2) are given by moments on sub-simplexes. Now we present a set of DoFs as function values on the interpolation points and give its dual basis for the  $k$ -th order Lagrange element on an  $n$ -simplex.

**Lemma 3.1** (Lagrange interpolation basis functions [29]). *A basis function of the  $k$ -th order Lagrange finite element space on  $T$  is:*

$$\phi_\alpha(\mathbf{x}) = \frac{1}{\alpha!} \prod_{i=0}^n \prod_{j=0}^{\alpha_i-1} (k\lambda_i(\mathbf{x}) - j), \quad \alpha \in \mathbb{T}_k^n,$$

with the DoFs defined as the function value at the interpolation points:

$$N_\alpha(u) = u(\mathbf{x}_\alpha), \quad \mathbf{x}_\alpha \in \mathcal{X}_T.$$

*Proof.* It is straightforward to verify the duality of the basis and DoFs

$$N_\beta(\phi_\alpha) = \phi_\alpha(\mathbf{x}_\beta) = \delta_{\alpha,\beta} = \begin{cases} 1 & \text{if } \alpha = \beta \\ 0 & \text{otherwise} \end{cases}.$$

As

$$|\mathbb{T}_k^n| = \binom{n+k}{k} = \dim \mathbb{P}_k(T),$$

$\{\phi_\alpha, \alpha \in \mathbb{T}_k^n\}$  is a basis of  $\mathbb{P}_k(T)$  and  $\{N_\alpha, \alpha \in \mathbb{T}_k^n\}$  is a basis of the dual space  $\mathbb{P}_k^*(T)$ .  $\square$

Given a triangulation  $\mathcal{T}_h$  and degree  $k$ , recall that

$$\mathcal{X}_{\mathcal{T}_h} = \bigcup_{T \in \mathcal{T}_h} \mathcal{X}_T = \bigoplus_{\ell=0}^n \bigoplus_{f \in \Delta_\ell(\mathcal{T}_h)} \mathcal{X}_f.$$

Denote by

$$\mathbb{T}_k^n(\mathcal{T}_h) := \bigoplus_{x_i \in \Delta_0(\mathcal{T}_h)} \mathbb{T}_k^0(x_i) \oplus \bigoplus_{\ell=1}^n \bigoplus_{f \in \Delta_\ell(\mathcal{T}_h)} \mathbb{T}_k^\ell(f).$$

For a lattice  $\alpha \in \mathbb{T}_k^\ell(\mathring{f})$ , we use extension operator  $E$  defined in (2.1) to extend  $\alpha$  to each simplex  $T$  containing  $f$ . We also extend the polynomial on  $f$  to  $T$  by the Bernstein form.

**Theorem 3.2** (DoFs of Lagrange finite element on  $\mathcal{T}_h$ ). *A basis for the  $k$ -th Lagrange finite element space  $V_k^L(\mathcal{T}_h)$  is*

$$\{\phi_\alpha, \alpha \in \mathbb{T}_k^n(\mathcal{T}_h)\}$$

with DoFs

$$N_\alpha(u) = u(x_\alpha), \quad x_\alpha \in \mathcal{X}_{\mathcal{T}_h}.$$

*Proof.* For  $F \in \Delta_{n-1}(\mathcal{T}_h)$ , thanks to Lemma 3.1,  $\phi_\alpha|_F$  is uniquely determined by DoFs  $\{u(x_\alpha), x_\alpha \in \mathcal{X}_F\}$  on face  $F$ , hence  $\phi_\alpha \in V_k^L(\mathcal{T}_h)$ . Clearly the cardinality of  $\{\phi_\alpha, \alpha \in \mathbb{T}_k^n(\mathcal{T}_h)\}$  is same as the dimension of space  $V_k^L(\mathcal{T}_h)$ . Then we only need to show these functions are linearly independent, which follows from the fact  $N_\beta(\phi_\alpha) = \phi_\alpha(x_\beta) = \delta_{\alpha,\beta}$  for  $\alpha, \beta \in \mathbb{T}_k^n(\mathcal{T}_h)$ .  $\square$

We now generalize the basis for a scalar Lagrange element to a vector Lagrange element. For an interpolation point  $x \in \mathcal{X}_T$ , let  $\{e_i^x, i=0, \dots, n-1\}$  be a basis of  $\mathbb{R}^n$ , and its dual basis is denoted by  $\{\hat{e}_i^x, i=0, \dots, n-1\}$ , i.e.,

$$(\hat{e}_i^x, e_j^x) = \delta_{i,j}.$$

When  $\{e_i^x, i=0, \dots, n-1\}$  is orthonormal, its dual basis is itself.

**Corollary 3.3.** A polynomial function  $u \in \mathbb{P}_k^n(T)$  can be uniquely determined by the DoFs:

$$N_\alpha^i(u) := u(x_\alpha) \cdot e_i^{x_\alpha}, \quad x_\alpha \in \mathcal{X}_T, i=0, \dots, n-1.$$

The basis function on  $T$  dual to this set of DoFs can be explicitly written as:

$$\phi_\alpha^i(x) = \phi_\alpha(x) \hat{e}_i^{x_\alpha}, \quad \alpha \in \mathbb{T}_k^n, i=0, \dots, n-1.$$

*Proof.* It is straightforward to verify the duality

$$N_\beta^j(\phi_\alpha^i) = \phi_\alpha^i(x_\beta) \cdot e_j^{x_\beta} = \phi_\alpha(x_\beta) \hat{e}_i^{x_\alpha} \cdot e_j^{x_\beta} = \delta_{i,j} \delta_{\alpha,\beta},$$

for  $\alpha, \beta \in \mathbb{T}_k^n, i, j=0, \dots, n-1$ .  $\square$

If the basis  $\{e_i^f, i=0, \dots, n-1\}$  is global in the sense that it is independent of element  $T$  containing  $x$ , we get the continuous vector Lagrange elements. Choose different basis will give different continuity.

## 4 Geometric Decompositions of Face Elements

Define  $H(\operatorname{div}, \Omega) := \{v \in L^2(\Omega; \mathbb{R}^n) : \operatorname{div} v \in L^2(\Omega)\}$ . For a subdomain  $K \subseteq \Omega$ , the trace operator for the div operator is

$$\operatorname{tr}_K^{\operatorname{div}} v = \mathbf{n} \cdot \mathbf{v}|_{\partial K} \quad \text{for } v \in H(\operatorname{div}, \Omega),$$

where  $\mathbf{n}$  denotes the outwards unit normal vector of  $\partial K$ . Given a triangulation  $\mathcal{T}_h$  and a piecewise smooth function  $\mathbf{u}$ , it is well known that  $\mathbf{u} \in H(\operatorname{div}, \Omega)$  if and only if  $\mathbf{n}_F \cdot \mathbf{u}$  is continuous across all faces  $F \in \Delta_{n-1}(\mathcal{T}_h)$ , which can be ensured by having DoFs on faces. An  $H(\operatorname{div})$ -conforming finite element is thus also called a face element.

### 4.1 Geometric decomposition

Define the polynomial div bubble space

$$\mathbb{B}_k(\operatorname{div}, T) = \ker(\operatorname{tr}_T^{\operatorname{div}}) \cap \mathbb{P}_k^n(T).$$

Recall that  $\mathbb{B}_k^\ell(f) = \mathbb{B}_k(f) \otimes \mathcal{T}^f$  consists of bubble polynomials on the tangential plane of  $f$ . For  $\mathbf{u} \in \mathbb{B}_k^\ell(f)$ , as  $\mathbf{u}$  is on the tangential plane,  $\mathbf{u} \cdot \mathbf{n}_F = 0$  for  $f \subseteq F$ . When  $f \not\subseteq F$ ,  $b_f|_F = 0$ . So  $\mathbb{B}_k^\ell(f) \subseteq \mathbb{B}_k(\operatorname{div}, T)$  for  $k \geq 2$  and  $\dim f \geq 1$ . In [16], we have proved that the div-bubble polynomial space has the following decomposition.

**Lemma 4.1.** *For  $k \geq 2$ ,*

$$\mathbb{B}_k(\operatorname{div}, T) = \bigoplus_{\ell=1}^n \bigoplus_{f \in \Delta_\ell(T)} \mathbb{B}_k^\ell(f).$$

Notice that as no tangential plane on vertices, there is no div-bubble associated to vertices and consequently the degree of a div-bubble polynomial is greater than or equal to 2. Next we present two geometric decompositions of a div-element.

**Theorem 4.1.** *For  $k \geq 1$ , we have*

$$\mathbb{P}_k^n(T) = \mathbb{P}_1^n(T) \oplus \left( \bigoplus_{\ell=1}^{n-1} \bigoplus_{f \in \Delta_\ell(T)} (\mathbb{B}_k(f) \otimes \mathcal{N}^f) \right) \oplus \mathbb{B}_k(\operatorname{div}, T), \quad (4.1)$$

$$\mathbb{P}_k^n(T) = \left( \bigoplus_{F \in \Delta_{n-1}(T)} (\mathbb{P}_k(F) \mathbf{n}_F) \right) \oplus \mathbb{B}_k(\operatorname{div}, T). \quad (4.2)$$

*Proof.* The first decomposition (4.1) is a rearrangement of (3.5) by merging the tangential component  $\mathbb{B}_k^\ell(f)$  into the bubble space  $\mathbb{B}_k(\operatorname{div}, T)$ .

Next we prove the decomposition (4.2). For an  $\ell$ -dimensional,  $0 \leq \ell \leq n-1$ , sub-simplex  $f \in \Delta_\ell(T)$ , we choose the  $n-\ell$  face normal vectors  $\{\mathbf{n}_F : F \in \Delta_{n-1}(T), f \subseteq F\}$  as the basis of  $\mathcal{N}^f$ . Therefore we have

$$\mathbb{B}_k(f) \otimes \mathcal{N}^f = \bigoplus_{F \in \Delta_{n-1}(T), f \subseteq F} \mathbb{B}_k(f) \mathbf{n}_F.$$

Then (4.1) becomes

$$\mathbb{P}_k^n(T) = \mathbb{P}_1^n(T) \oplus \left( \bigoplus_{\ell=1}^{n-1} \bigoplus_{f \in \Delta_\ell(T)} \bigoplus_{F \in \Delta_{n-1}(T), f \subseteq F} \mathbb{B}_k(f) \mathbf{n}_F \right) \oplus \mathbb{B}_k(\operatorname{div}, T).$$

At a vertex  $v$ , we choose  $\{\mathbf{n}_F : F \in \Delta_{n-1}(T), v \subseteq F\}$  as the basis of  $\mathbb{R}^n$  and write

$$\begin{aligned}\mathbb{P}_1^n(T) &= \bigoplus_{x \in \Delta_0(T)} \bigoplus_{F \in \Delta_{n-1}(T), x \in \Delta_0(F)} \text{span}\{\lambda_x \mathbf{n}_F\} \\ &= \bigoplus_{F \in \Delta_{n-1}(T)} \bigoplus_{x \in \Delta_0(F)} \text{span}\{\lambda_x \mathbf{n}_F\} \\ &= \bigoplus_{F \in \Delta_{n-1}(T)} \mathbb{P}_1(F) \mathbf{n}_F.\end{aligned}$$

Then by swapping the ordering of  $f$  and  $F$  in the direct sum, i.e.,

$$\bigoplus_{\ell=1}^{n-1} \bigoplus_{f \in \Delta_\ell(T)} \bigoplus_{F \in \Delta_{n-1}(T), f \subseteq F} \rightarrow \bigoplus_{F \in \Delta_{n-1}(T)} \bigoplus_{\ell=1}^{n-1} \bigoplus_{f \in \Delta_\ell(F)},$$

and using the decomposition (3.1) of Lagrange element, we obtain the decomposition (4.2).  $\square$

In decomposition (4.1), we single out  $\mathbb{P}_1^n(T)$  to emphasize an  $H(\text{div})$ -conforming element can be obtained by adding div-bubble and normal component on sub-simplexes starting from edges. In (4.2), we group all normal components facewisely which leads to the classical BDM element.

As  $H(\text{div}, \Omega)$ -conforming elements require the normal continuity across each  $F$ , the normal vector  $\mathbf{n}_F$  is chosen globally. Namely  $\mathbf{n}_F$  depends on  $F$  only. It may coincide with the outwards or inwards normal vector for an element  $T$  containing  $F$ . On the contrary, all tangential basis for  $\mathcal{T}^f$  are local and thus the tangential component are multi-valued and merged to the element-wise div bubble function  $\mathbb{B}_k(\text{div}, T)$ .

## 4.2 A nodal basis for the BDM element

For the efficient implementation, we employ the DoFs of the function values at interpolation nodes and combine with  $t-n$  decompositions to present a nodal basis for the BDM element.

Given an  $f \in \Delta_\ell(T)$ , we choose  $\{\mathbf{n}_F, F \in \Delta_{n-1}(T), f \subseteq F\}$  as the basis for its normal plane  $\mathcal{N}^f$  and an arbitrary basis  $\{\mathbf{t}_i^f, i=1, \dots, \ell\}$  for the tangential plane. We shall choose  $\{\hat{\mathbf{n}}_{F_i} \in \mathcal{N}^f, i \in f^*\}$  a basis of  $\mathcal{N}^f$  dual to  $\{\mathbf{n}_{F_i} \in \mathcal{N}^f, i \in f^*\}$ , i.e.,

$$(\mathbf{n}_F, \hat{\mathbf{n}}_{F'}) = \delta_{F, F'}, \quad F, F' \in \Delta_{n-1}(T), f \in F \cap F'.$$

Similarly choose a basis  $\{\hat{\mathbf{t}}_i^f\}$  dual to  $\{\mathbf{t}_i^f\}$ .

We can always choose an orthonormal basis for the tangential plane  $\mathcal{T}^f$  but for the normal plane  $\mathcal{N}^f$  with basis  $\{\mathbf{n}_{F_i} \in \mathcal{N}^f, i \in f^*\}$ , we use Lemma 4.2 to find its dual basis.

For  $f \in \Delta_\ell(T)$  and  $e \in \partial f$ , let  $\mathbf{n}_f^e$  be a unit normal vector of  $e$  but tangential to  $f$ . When  $\ell=1$ ,  $f$  is an edge and  $e$  is a vertex. Then  $\mathbf{n}_f^e$  is the edge vector of  $f$ . Using these notations we can give an explicit expression of the dual basis  $\{\hat{\mathbf{n}}_{F_i} \in \mathcal{N}^f, i \in f^*\}$ .

**Lemma 4.2.** For  $f \in \Delta_\ell(T)$ ,

$$\{\hat{\mathbf{n}}_{F_i} = \frac{1}{\mathbf{n}_{f+i}^f \cdot \mathbf{n}_{F_i}} \mathbf{n}_{f+i}^f \quad i \in f^*\}, \quad (4.3)$$

where  $f+i$  denotes the  $(\ell+1)$ -dimensional face in  $\Delta_{\ell+1}(T)$  with vertices  $f(0), \dots, f(\ell)$  and  $i$  for  $i \in f^*$ , is a basis of  $\mathcal{N}^f$  dual to  $\{\mathbf{n}_{F_i} \in \mathcal{N}^f, i \in f^*\}$ .

*Proof.* Clearly  $\mathbf{n}_{f+i}^f \in \mathcal{N}^f$  for  $i \in f^*$ . It suffices to prove

$$\mathbf{n}_{f+i}^f \cdot \mathbf{n}_{F_j} = 0 \quad \text{for } i, j \in f^*, i \neq j,$$

which follows from  $\mathbf{n}_{f+i}^f \in \mathcal{T}^{f+i}$  and  $f+i \subseteq F_j$ .  $\square$

By Corollary 3.3, we obtain a nodal basis for BDM face elements.

**Theorem 4.2.** For each  $f \in \Delta_\ell(T)$ , we choose  $\{\mathbf{e}_i^f, i=0, \dots, n-1\} = \{\mathbf{t}_i^f, i=1, \dots, \ell, \mathbf{n}_{F_i}, i \in f^*\}$  and its dual basis  $\{\hat{\mathbf{e}}_i^f, i=0, \dots, n-1\} = \{\hat{\mathbf{t}}_i^f, i=1, \dots, \ell, \hat{\mathbf{n}}_{F_i}, i \in f^*\}$ . A basis function of the  $k$ -th order BDM element space on  $T$  is:

$$\{\phi_\alpha(\mathbf{x})\hat{\mathbf{e}}_i^f, i=0, 1, \dots, n-1, \alpha \in \mathbb{T}_k^\ell(f)\}_{f \in \Delta_\ell(T), \ell=0, 1, \dots, n},$$

with the DoFs at the interpolation points defined as:

$$\{u(\mathbf{x}_\alpha)\mathbf{e}_i^f, i=0, 1, \dots, n-1, \mathbf{x}_\alpha \in \mathcal{X}_f\}_{f \in \Delta_\ell(T), \ell=0, 1, \dots, n}. \quad (4.4)$$

By choosing a global normal basis in the sense that  $\mathbf{n}_F$  depending only on  $F$  not the element containing  $F$ , we impose the continuity on the normal direction. We choose a local  $\mathbf{t}^f$ , i.e., for different element  $T$  containing  $f$ ,  $\phi_\alpha(\mathbf{x})\mathbf{t}^f(T)$  is different, then no continuity is imposed for the tangential direction.

Define the global finite element space

$$V_h^{\text{div}} := \{\mathbf{u} \in L^2(\Omega; \mathbb{R}^n) : \mathbf{u}|_T \in \mathbb{P}_k(T; \mathbb{R}^n) \text{ for each } T \in \mathcal{T}_h, \\ \text{all the DoFs } u(\mathbf{x}_\alpha)\mathbf{n}_F \text{ in (4.4) across } F \in \Delta_{n-1}(\mathcal{T}_h) \text{ are single-valued}\}.$$

By Theorem 4.1,  $V_h^{\text{div}} \subset H(\text{div}, \Omega)$  and is equivalent to the BDM space.

The novelty is that we only need a basis of Lagrange element which is well documented; see Section 3.2. Coupling with different  $t-n$  decomposition at different sub-simplex, we obtain the classical face elements. This concept has been explored in the works of [20, 21] and [13], focusing on the implementation of the  $H(\text{div})$  element in two and three dimensions. Additionally, the adaptation of a 2D  $H(\text{curl})$  element through rotation is discussed in [20, 21]. As we will demonstrate in the subsequent section, extending the edge element to higher dimensions presents significant challenges. This extension necessitates a comprehensive characterization of the curl operator and its associated polynomial bubble space.

## 5 Geometric Decompositions of Edge Elements

In this section we present geometric decompositions of  $H(\text{curl})$ -conforming finite element space on an  $n$ -dimensional simplex. We first generalize the curl differential operator to  $n$  dimensions and study its trace which motivates our decomposition. We then give an explicit basis dual to function values at interpolation points.

### 5.1 Differential operator and its trace

Denote by  $\mathbb{S}$  and  $\mathbb{K}$  the subspace of symmetric matrices and skew-symmetric matrices of  $\mathbb{R}^{n \times n}$ , respectively. For a smooth vector function  $\mathbf{v}$ , define

$$\operatorname{curl} \mathbf{v} := 2\operatorname{skw}(\operatorname{grad} \mathbf{v}) = \operatorname{grad} \mathbf{v} - (\operatorname{grad} \mathbf{v})^\top,$$

which is a skew-symmetric matrix function. In two dimensions, for  $\mathbf{v} = (v_1, v_2)^\top$ ,

$$\operatorname{curl} \mathbf{v} = \begin{pmatrix} 0 & \partial_{x_2} v_1 - \partial_{x_1} v_2 \\ \partial_{x_1} v_2 - \partial_{x_2} v_1 & 0 \end{pmatrix} = \operatorname{mskw}(\operatorname{rot} \mathbf{v}),$$

where  $\operatorname{mskw} \mathbf{u} := \begin{pmatrix} 0 & -u \\ u & 0 \end{pmatrix}$  and  $\operatorname{rot} \mathbf{v} := \partial_{x_1} v_2 - \partial_{x_2} v_1$ . In three dimensions, for  $\mathbf{v} = (v_1, v_2, v_3)^\top$ ,

$$\operatorname{curl} \mathbf{v} = \begin{pmatrix} 0 & \partial_{x_2} v_1 - \partial_{x_1} v_2 & \partial_{x_3} v_1 - \partial_{x_1} v_3 \\ \partial_{x_1} v_2 - \partial_{x_2} v_1 & 0 & \partial_{x_3} v_2 - \partial_{x_2} v_3 \\ \partial_{x_1} v_3 - \partial_{x_3} v_1 & \partial_{x_2} v_3 - \partial_{x_3} v_2 & 0 \end{pmatrix} = \operatorname{mskw}(\nabla \times \mathbf{v}),$$

where  $\operatorname{mskw} \mathbf{u} := \begin{pmatrix} 0 & -u_3 & u_2 \\ u_3 & 0 & -u_1 \\ -u_2 & u_1 & 0 \end{pmatrix}$  with  $\mathbf{u} = (u_1, u_2, u_3)^\top$ . Hence we can identify  $\operatorname{curl} \mathbf{v}$

as scalar  $\operatorname{rot} \mathbf{v}$  in two dimensions, and vector  $\nabla \times \mathbf{v}$  in three dimensions. In general,  $\operatorname{curl} \mathbf{u}$  is understood as a skew-symmetric matrix.

Define Sobolev space

$$H(\operatorname{curl}, \Omega) := \{\mathbf{v} \in L^2(\Omega; \mathbb{R}^n) : \operatorname{curl} \mathbf{v} \in L^2(\Omega; \mathbb{K})\}.$$

Given a face  $F \in \Delta_{n-1}(T)$ , define the trace operator of  $\operatorname{curl}$  as

$$\operatorname{tr}_F^{\operatorname{curl}} \mathbf{v} = 2\operatorname{skw}(\mathbf{v} \mathbf{n}_F^\top)|_F = (\mathbf{v} \mathbf{n}_F^\top - \mathbf{n}_F \mathbf{v}^\top)|_F.$$

We define  $\operatorname{tr}^{\operatorname{curl}}$  as a piecewise defined operator as

$$(\operatorname{tr}^{\operatorname{curl}} \mathbf{v})|_F = \operatorname{tr}_F^{\operatorname{curl}} \mathbf{v}, \quad F \in \Delta_{n-1}(T).$$

For a vector  $\mathbf{v} \in \mathbb{R}^n$  and an  $n-1$  dimensional face  $F$ , the tangential part of  $\mathbf{v}$  on  $F$  is

$$\Pi_F \mathbf{v} := \mathbf{v}|_F - (\mathbf{v}|_F \cdot \mathbf{n}_F) \mathbf{n}_F = \sum_{i=1}^{n-1} (\mathbf{v}|_F \cdot \mathbf{t}_i^F) \mathbf{t}_i^F,$$

where  $\{\mathbf{t}_i^F, i=1, \dots, n-1\}$  is an orthonormal basis of  $F$ . As we treat  $\operatorname{curl} \mathbf{v}$  as a matrix, so is the trace  $\operatorname{tr}_F^{\operatorname{curl}} \mathbf{v}$ , while the tangential component of  $\mathbf{v}$  is a vector. Their relation is given in the following lemma.

**Lemma 5.1.** For face  $F \in \Delta_{n-1}(T)$ , we have

$$\text{tr}_F^{\text{curl}} \mathbf{v} = 2\text{skw}((\Pi_F \mathbf{v}) \mathbf{n}_F^\top), \quad \Pi_F \mathbf{v} = (\text{tr}_F^{\text{curl}} \mathbf{v}) \mathbf{n}_F. \quad (5.1)$$

*Proof.* By the decomposition  $\mathbf{v}|_F = \Pi_F \mathbf{v} + (\mathbf{v}|_F \cdot \mathbf{n}_F) \mathbf{n}_F$ ,

$$\text{tr}_F^{\text{curl}} \mathbf{v} = 2\text{skw}((\Pi_F \mathbf{v}) \mathbf{n}_F^\top + (\mathbf{v}|_F \cdot \mathbf{n}_F) \mathbf{n}_F \mathbf{n}_F^\top) = 2\text{skw}((\Pi_F \mathbf{v}) \mathbf{n}_F^\top),$$

which implies the first identity. Then by  $\mathbf{n}_F^\top \mathbf{n}_F = 1$  and  $(\Pi_F \mathbf{v})^\top \mathbf{n}_F = 0$ ,

$$(\text{tr}_F^{\text{curl}} \mathbf{v}) \mathbf{n}_F = ((\Pi_F \mathbf{v}) \mathbf{n}_F^\top - \mathbf{n}_F (\Pi_F \mathbf{v})^\top) \mathbf{n}_F = \Pi_F \mathbf{v},$$

i.e. the second identity holds.  $\square$

Thanks to (5.1), the vanishing tangential part  $\Pi_F \mathbf{v}$  and the vanishing tangential trace  $(\text{tr}_F^{\text{curl}} \mathbf{v})$  are equivalent.

**Lemma 5.2.** Let  $\mathbf{v} \in L^2(\Omega; \mathbb{R}^n)$  and  $\mathbf{v}|_T \in H^1(T; \mathbb{S})$  for each  $T \in \mathcal{T}_h$ . Then  $\mathbf{v} \in H(\text{curl}, \Omega)$  if and only if  $\Pi_F \mathbf{v}|_{T_1} = \Pi_F \mathbf{v}|_{T_2}$  for all interior face  $F \in \Delta_{n-1}(\mathcal{T}_h)$ , where  $T_1$  and  $T_2$  are two elements sharing  $F$ .

*Proof.* It is an immediate result of Lemma 5.1 in [7] and (5.1).  $\square$

## 5.2 Polynomial bubble space

Define the polynomial bubble space for the curl operator as

$$\mathbb{B}_k(\text{curl}, T) = \ker(\text{tr}^{\text{curl}}) \cap \mathbb{P}_k^n(T).$$

For Lagrange bubble space  $\mathbb{B}_k^n(T)$ , all components of the vector function vanish on  $\partial T$  and consequently on all sub-simplex with dimension  $\leq n-1$ . For  $\mathbf{u} \in \mathbb{B}_k(\text{curl}, T)$ , only the tangential component vanishes, which will imply  $\mathbf{u}$  vanishes on sub-simplex with dimension  $\leq n-2$ .

**Lemma 5.3.** For  $\mathbf{u} \in \mathbb{B}_k(\text{curl}, T)$ , it holds  $\mathbf{u}|_f = \mathbf{0}$  for all  $f \in \Delta_\ell(T), 0 \leq \ell \leq n-2$ . Consequently  $\mathbb{B}_k(\text{curl}, T) \subset \mathbb{B}_k^n(T) \oplus \bigoplus_{F \in \Delta_{n-1}(T)} \mathbb{B}_k^n(F)$ .

*Proof.* It suffices to consider a sub-simplex  $f \in \Delta_{n-2}(T)$ . Let  $F_1, F_2 \in \Delta_{n-1}(T)$  such that  $f = F_1 \cap F_2$ . By  $\text{tr}_{F_i}^{\text{curl}} \mathbf{u} = \mathbf{0}$  for  $i=1,2$ , we have  $\Pi_{F_i} \mathbf{u} = \mathbf{0}$  and consequently

$$(\mathbf{u} \cdot \mathbf{t}_i^f)|_f = 0, \quad (\mathbf{u} \cdot \mathbf{n}_{F_1}^f)|_f = (\mathbf{u} \cdot \mathbf{n}_{F_2}^f)|_f = 0 \quad \text{for } i=1, \dots, n-2,$$

where  $\mathbf{n}_{F_i}^f$  is a normal vector  $f$  sitting on  $F_i$ . As  $\text{span}\{\mathbf{t}_1^f, \dots, \mathbf{t}_{n-2}^f, \mathbf{n}_{F_1}^f, \mathbf{n}_{F_2}^f\} = \mathbb{R}^n$ , we acquire  $\mathbf{u}|_f = \mathbf{0}$ . By the property of face bubbles, we conclude  $\mathbf{u}$  is a linear combination of element bubble and  $n-1$  face bubbles.  $\square$

Obviously  $\mathbb{B}_k^n(T) \subset \mathbb{B}_k(\text{curl}, T)$ . As  $\text{tr}^{\text{curl}}$  contains the tangential component only, the normal component  $\mathbb{B}_k(F)\mathbf{n}_F$  is also a curl bubble. The following result says their sum is precisely all curl bubble polynomials.

**Theorem 5.1.** *For  $k \geq 1$ , it holds that*

$$\mathbb{B}_k(\text{curl}, T) = \mathbb{B}_k^n(T) \oplus \bigoplus_{F \in \Delta_{n-1}(T)} \mathbb{B}_k(F)\mathbf{n}_F, \quad (5.2)$$

and

$$\text{tr}^{\text{curl}} : \mathbb{P}_1^n(T) \oplus \bigoplus_{\ell=1}^{n-2} \bigoplus_{f \in \Delta_\ell(T)} \mathbb{B}_k^n(f) \oplus \bigoplus_{F \in \Delta_{n-1}(T)} \mathbb{B}_k^{n-1}(F) \rightarrow \text{tr}^{\text{curl}} \mathbb{P}_k^n(T) \quad (5.3)$$

is a bijection.

*Proof.* It is obvious that

$$\mathbb{B}_k^n(T) \oplus \bigoplus_{F \in \Delta_{n-1}(T)} \mathbb{B}_k(F)\mathbf{n}_F \subseteq \mathbb{B}_k(\text{curl}, T).$$

Then apply the trace operator to the decomposition (3.5) to conclude that the map  $\text{tr}^{\text{curl}}$  in (5.3) is onto.

Now we prove it is also injective. Take a function  $\mathbf{u} \in \mathbb{P}_1^n(T) \oplus \bigoplus_{\ell=1}^{n-2} \bigoplus_{f \in \Delta_\ell(T)} \mathbb{B}_k^n(f) \oplus \bigoplus_{F \in \Delta_{n-1}(T)} \mathbb{B}_k^{n-1}(F)$  and  $\text{tr}^{\text{curl}} \mathbf{u} = \mathbf{0}$ . By Lemma 5.3, we can assume  $\mathbf{u} = \sum_{F \in \Delta_{n-1}(T)} \mathbf{u}_k^F$  with  $\mathbf{u}_k^F \in \mathbb{B}_k^{n-1}(F)$ . Take  $F \in \Delta_{n-1}(T)$ . We have  $\mathbf{u}|_F = \mathbf{u}_k^F|_F \in \mathbb{B}_k^{n-1}(F)$ . Hence  $(\mathbf{u}_k^F \cdot \mathbf{t})|_F = (\mathbf{u} \cdot \mathbf{t})|_F = 0$  for any  $\mathbf{t} \in \mathcal{T}^F$ , which results in  $\mathbf{u}_k^F = \mathbf{0}$ . Therefore  $\mathbf{u} = \mathbf{0}$ .

Once we have proved the map  $\text{tr}$  in (5.3) is bijection, we conclude (5.2) from the decomposition (3.5).  $\square$

We will use  $\text{curl}_f$  to denote the curl operator restricted to a sub-simplex  $f$  with  $\dim f \geq 1$ . For  $f \in \Delta_\ell(T), \ell = 2, \dots, n-1$ , by applying Theorem 5.1 to  $f$ , we have

$$\mathbb{B}_k(\text{curl}_f, f) = \mathbb{B}_k^\ell(f) \oplus \bigoplus_{e \in \partial f} \mathbb{B}_k(e)\mathbf{n}_f^e. \quad (5.4)$$

Notice that the  $\text{curl}_f$ -bubble function is defined for  $\ell \geq 2$  not including edges. Indeed, for an edge  $e$  and a vertex  $x$  of  $e$ ,  $\mathbf{n}_e^x$  is  $\mathbf{t}_e$  if  $x$  is the ending vertex of  $e$  and  $-\mathbf{t}_e$  otherwise. Then for  $\ell = 1$

$$\mathbb{B}_k(e)\mathbf{t}_e \oplus \bigoplus_{x \in \partial e} \text{span}\{\lambda_x \mathbf{n}_e^x\} = \mathbb{P}_k(e)\mathbf{t}_e. \quad (5.5)$$

which is the full polynomial not vanishing on  $\partial e$ .

### 5.3 Geometric decompositions

For  $e \in \Delta_\ell(T)$ , we choose the basis  $\{\mathbf{n}_f^e : f = e + i, i \in e^*\}$  for  $\mathcal{N}^e$  and a basis  $\{\mathbf{t}_i^e, i = 1, \dots, \ell\}$  for  $\mathcal{T}^e$ . So we have the following geometric decompositions of  $\mathbb{P}_k^n(T)$ .



**Theorem 5.2.** For  $k \geq 1$ , we have

$$\mathbb{P}_k^n(T) = \mathbb{P}_1^n(T) \oplus \bigoplus_{\ell=1}^n \bigoplus_{e \in \Delta_\ell(T)} \mathbb{B}_k(e) \otimes \text{span}\{\mathbf{t}_i^e\}_{i=1}^\ell \oplus \mathbb{B}_k(e) \otimes \text{span}\{\mathbf{n}_{e+i}^e, i \in e^*\}, \quad (5.6)$$

$$\mathbb{P}_k^n(T) = \bigoplus_{e \in \Delta_1(T)} \mathbb{P}_k(e) \mathbf{t}_e \oplus \bigoplus_{\ell=2}^n \bigoplus_{f \in \Delta_\ell(T)} \mathbb{B}_k(\text{curl}_f, f). \quad (5.7)$$

*Proof.* Decomposition (5.6) is the component form of decomposition (3.5). We can write  $\mathbb{B}_k(e) \otimes \text{span}\{\mathbf{n}_{e+i}^e, i \in e^*\} = \bigoplus_{f \in \Delta_{\ell+1}(T), e \subseteq f} \mathbb{B}_k(e) \mathbf{n}_f^e$ . Then in the summation (5.6), we shift the normal component one level up and switch the sum of  $e$  and  $f$ :

$$\begin{aligned} & \bigoplus_{\ell=1}^n \bigoplus_{e \in \Delta_\ell(T)} [\mathbb{B}_k^\ell(e) \oplus \bigoplus_{f \in \Delta_{\ell+1}(T), e \subseteq f} \mathbb{B}_k(e) \mathbf{n}_f^e] \\ &= \bigoplus_{e \in \Delta_1(T)} \mathbb{B}_k(e) \mathbf{t}_e \oplus \bigoplus_{\ell=2}^n \bigoplus_{f \in \Delta_\ell(T)} [\mathbb{B}_k^\ell(f) \oplus \bigoplus_{e \subseteq \partial f} \mathbb{B}_k(e) \mathbf{n}_f^e]. \end{aligned}$$

Then by the characterization (5.4) of  $\mathbb{B}_k(\text{curl}_f, f)$  and (5.5), we get the decomposition (5.7).  $\square$

Decomposition (5.7) is the counterpart of (3.3) for Lagrange element.

#### 5.4 Tangential-Normal decomposition of the second family of edge elements

Recall that for  $e \in \Delta_{\ell-1}(T)$ , the basis  $\{\mathbf{n}_f^e : f \in \Delta_\ell(T), e \subseteq f\}$  of  $\mathcal{N}^e$  is dual to the basis  $\{\mathbf{n}_F : F \in \Delta_{n-1}(T), e \subseteq F\}$ ; see Lemma 4.2.

**Theorem 5.3.** Take  $\mathbb{P}_k^n(T)$  as the shape function space. Then it is determined by the following DoFs

$$\int_e \mathbf{u} \cdot \mathbf{t} \, p \, ds, \quad p \in \mathbb{P}_k(e), e \in \Delta_1(T), \quad (5.8a)$$

$$\int_f \mathbf{u} \cdot \mathbf{p} \, ds, \quad \mathbf{p} \in \mathbb{B}_k(\text{curl}_f, f), f \in \Delta_\ell(T), \ell = 2, \dots, n \quad (5.8b)$$

*Proof.* Based on the decomposition (5.6), the shape function  $\mathbb{P}_k^n(T)$  is determined by the following DoFs

$$\int_e \mathbf{u} \cdot \mathbf{t} \, p \, ds, \quad p \in \mathbb{P}_k(e), e \in \Delta_1(T), \quad (5.9a)$$

$$\int_f (\mathbf{u} \cdot \mathbf{t}_i^f) \, p \, ds, \quad p \in \mathbb{P}_{k-(\ell+1)}(f), i = 1, \dots, \ell, \quad (5.9b)$$

$$\int_e (\mathbf{u} \cdot \mathbf{n}_f^e) \, p \, ds, \quad p \in \mathbb{P}_{k-\ell}(e), e \in \partial f \quad (5.9c)$$

for  $f \in \Delta_\ell(T), \ell = 2, \dots, n$ . By (5.2) and (5.4), DoFs (5.9) are equivalent to DoFs (5.8).  $\square$

**Remark 5.1.** The DoFs of the second kind Nédélec edge element in [7, 28] are

$$\begin{aligned} & \int_e \mathbf{u} \cdot \mathbf{t} \, p \, ds, \quad p \in \mathbb{P}_k(e), e \in \Delta_1(T), \\ & \int_f \mathbf{u} \cdot \mathbf{p} \, ds, \quad \mathbf{p} \in \mathbb{P}_{k-\ell}^\ell(f) + (\Pi_f \mathbf{x}) \mathbb{P}_{k-\ell}(f), f \in \Delta_\ell(T), \ell = 2, \dots, n. \end{aligned}$$

There is an isomorphism between  $\mathbb{P}_{k-\ell}^\ell(f) + (\Pi_f \mathbf{x})\mathbb{P}_{k-\ell}(f)$  and  $\mathbb{B}_k(\text{curl}_f, f)$  for  $f \in \Delta_\ell(T)$  with  $\ell = 2, \dots, n$ , that is  $\mathbb{B}_k(\text{curl}_f, f)$  is uniquely determined by DoF

$$\int_f \mathbf{u} \cdot \mathbf{p} \, ds, \quad \mathbf{p} \in \mathbb{P}_{k-\ell}^\ell(f) + (\Pi_f \mathbf{x})\mathbb{P}_{k-\ell}(f),$$

whose proof can be found in Lemma 4.7 in [7].  $\square$

Given an  $e \in \Delta_{\ell-1}(T_h)$ , we choose a global  $\{\mathbf{n}_f^e, e \subseteq f \in \Delta_\ell(T_h)\}$  as the basis for the normal plane  $\mathcal{N}^e$  and a global basis  $\{\mathbf{t}_i^e\}$  of  $\mathcal{T}^e$ . Define the global finite element space

$$V_h^{\text{curl}} := \{\mathbf{u} \in L^2(\Omega; \mathbb{R}^n) : \mathbf{u}|_T \in \mathbb{P}_k(T; \mathbb{R}^n) \text{ for each } T \in \mathcal{T}_h, \\ \text{all the DoFs (5.8) are single-valued}\}.$$

**Lemma 5.4.** *We have  $V_h^{\text{curl}} \subset H(\text{curl}, \Omega)$ .*

*Proof.* For an  $F \in \Delta_{n-1}(T)$ , DoFs (5.9) related to  $\Pi_F \mathbf{u}$  are

$$\int_e (\Pi_F \mathbf{u} \cdot \mathbf{t}_i^e) \, p \, ds, \quad i = 1, \dots, \ell-1, p \in \mathbb{P}_{k-\ell}(e), e \in \Delta_{\ell-1}(F), \ell = 2, \dots, n, \\ \int_e (\Pi_F \mathbf{u} \cdot \mathbf{n}_f^e) \, p \, ds, \quad f \in \Delta_\ell(F), e \subseteq f, p \in \mathbb{P}_{k-\ell}(e), e \in \Delta_{\ell-1}(F), \ell = 1, \dots, n-1,$$

thanks to DoFs (5.9), which uniquely determine  $\Pi_F \mathbf{u}$ .  $\square$

## 5.5 A nodal basis for the second-kind Nédélec edge element

By Corollary 3.3, we obtain a nodal basis for the second-kind Nédélec edge element.

**Theorem 5.4.** *For each  $e \in \Delta_\ell(T)$ ,  $\ell = 0, 1, \dots, n$ , we choose  $\{\mathbf{e}_i^e, i = 0, \dots, n-1\} = \{\mathbf{t}_i^e, i = 1, \dots, \ell, \mathbf{n}_f^e, f = e+i, i \in e^*\}$  and its dual basis  $\{\hat{\mathbf{e}}_i^e, i = 0, \dots, n-1\} = \{\hat{\mathbf{t}}_i^e, i = 1, \dots, \ell, \mathbf{n}_{F_i} / (\mathbf{n}_{F_i} \cdot \mathbf{n}_{e+i}^e), i \in e^*\}$ . A basis function of the  $k$ -th order second kind Nédélec edge element space on  $T$  is:*

$$\{\phi_\alpha(\mathbf{x}) \hat{\mathbf{e}}_i^e, i = 0, 1, \dots, n-1, \alpha \in \mathbb{T}_k^\ell(\hat{e})\}_{e \in \Delta_\ell(T), \ell = 0, 1, \dots, n},$$

with the DoFs at the interpolation points defined as:

$$\{u(\mathbf{x}_\alpha) \mathbf{e}_i^e, i = 0, 1, \dots, n-1, \mathbf{x}_\alpha \in \mathcal{X}_{\hat{e}}\}_{e \in \Delta_\ell(T), \ell = 0, 1, \dots, n}. \quad (5.10)$$

Notice that the basis  $\{\mathbf{t}_i^e\}$  depends only on  $e$  and  $\mathbf{n}_f^e$  depends on  $e$  and  $f$  but independent  $T$ . By asking the corresponding DoFs single valued, we obtain the tangential continuity. We can define the edge finite element space as

$$V_h^{\text{curl}} := \{\mathbf{u} \in L^2(\Omega; \mathbb{R}^n) : \mathbf{u}|_T \in \mathbb{P}_k(T; \mathbb{R}^n) \text{ for each } T \in \mathcal{T}_h, \text{ the DoFs } u(\mathbf{x}_\alpha) \mathbf{t}_i^e, u(\mathbf{x}_\alpha) \mathbf{n}_f^e \\ \text{in (5.10) are single-valued across all } e \text{ and } f \text{ with } \dim e, \dim f \leq n-1\}.$$

### 5.5.1 2D basis on triangular meshes

Let  $T$  be a triangle, for lattice point  $x$  located in different sub-simplices, we shall choose different frame  $\{e_x^0, e_x^1\}$  at  $x$  and its dual frame  $\{\hat{e}_x^0, \hat{e}_x^1\}$  as follows:

1. If  $x \in \Delta_0(T)$ , assume the two adjacent edges are  $e_0$  and  $e_1$ , then

$$e_x^0 = t_{e_0}, \quad e_x^1 = t_{e_1}, \quad \hat{e}_x^0 = \frac{n_{e_1}}{n_{e_1} \cdot t_{e_0}}, \quad \hat{e}_x^1 = \frac{n_{e_0}}{n_{e_0} \cdot t_{e_1}}.$$

2. If  $x \in \mathcal{X}_{\hat{e}}, e \in \Delta_1(T)$ , then

$$e_x^0 = t_e, \quad e_x^1 = n_e, \quad \hat{e}_x^0 = t_e, \quad \hat{e}_x^1 = n_e.$$

3. If  $x \in \mathcal{X}_T$ , then

$$e_x^0 = (1, 0), \quad e_x^1 = (0, 1), \quad \hat{e}_x^0 = (1, 0), \quad \hat{e}_x^1 = (0, 1).$$

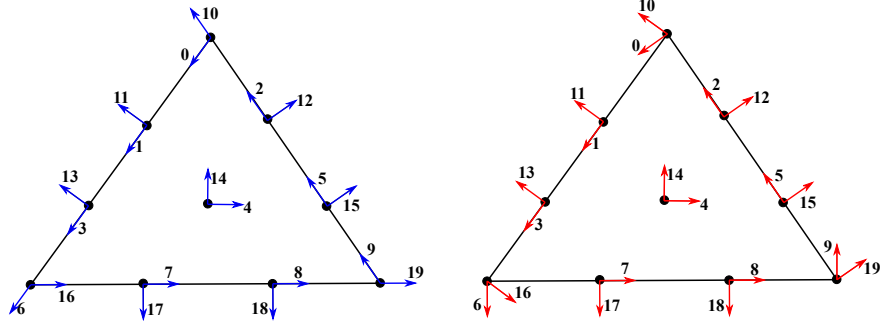


Figure 2: The left figure shows  $\{e_0, e_1\}$  at each interpolation point, the right figure shows  $\{\hat{e}_0, \hat{e}_1\}$  at each interpolation point.

### 5.5.2 3D basis on tetrahedron meshes

Let  $T$  be a tetrahedron, for any  $x \in \mathcal{X}_T$ , define a frame  $\{e_x^0, e_x^1, e_x^2\}$  at  $x$  and its dual frame  $\{\hat{e}_x^0, \hat{e}_x^1, \hat{e}_x^2\}$  as follows:

1. If  $x \in \Delta_0(T)$  and adjacent edges of  $x$  are  $e_0, e_1, e_2$ , adjacent faces of  $x$  are  $f_0, f_1, f_2$ , then

$$e_x^0 = t_{e_0}, \quad e_x^1 = t_{e_1}, \quad e_x^2 = t_{e_2},$$

$$\hat{e}_x^0 = \frac{n_{f_0}}{n_{f_0} \cdot t_{e_0}}, \quad \hat{e}_x^1 = \frac{n_{f_1}}{n_{f_1} \cdot t_{e_1}}, \quad \hat{e}_x^2 = \frac{n_{f_2}}{n_{f_2} \cdot t_{e_2}}.$$

2. If  $x \in \mathcal{X}_{\hat{e}}, e \in \Delta_1(T)$  and adjacent faces are  $f_0, f_1$  then

$$\begin{aligned} e_x^0 &= t_e, & e_x^1 &= n_{f_0} \times t_e, & e_x^2 &= n_{f_1} \times t_e, \\ \hat{e}_x^0 &= t_e, & \hat{e}_x^1 &= \frac{n_{f_1}}{n_{f_1} \cdot (n_{f_0} \times t_e)}, & \hat{e}_x^2 &= \frac{n_{f_0}}{n_{f_0} \cdot (n_{f_1} \times t_e)}. \end{aligned}$$

3. If  $x \in \mathcal{X}_{\hat{f}}, f \in \Delta_2(T)$ , the first edge of  $f$  is  $e$ , then

$$\begin{aligned} e_x^0 &= t_e, & e_x^1 &= t_e \times n_f, & e_x^2 &= n_f, \\ \hat{e}_x^0 &= t_e, & \hat{e}_x^1 &= t_e \times n_f, & \hat{e}_x^2 &= n_f. \end{aligned}$$

4. If  $x \in \mathcal{X}_{\hat{T}}$ , then

$$\begin{aligned} e_x^0 &= (1, 0, 0), & e_x^1 &= (0, 1, 0), & e_x^2 &= (0, 0, 1), \\ \hat{e}_x^0 &= (1, 0, 0), & \hat{e}_x^1 &= (0, 1, 0), & \hat{e}_x^2 &= (0, 0, 1). \end{aligned}$$

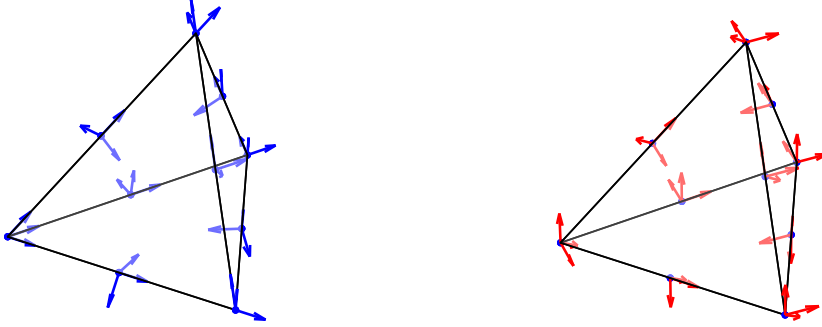


Figure 3: The left figure shows  $\{e_0, e_1, e_2\}$  at each interpolation point, the right figure shows  $\{\hat{e}_0, \hat{e}_1, \hat{e}_2\}$  at each interpolation point.

## 6 Indexing Management of Degrees of Freedom

In Section 2, we have already discussed the dictionary indexing rule for interpolation points in each element. In this section, we will address the global indexing rules for Lagrange interpolation points, ensuring that interpolation points on a sub-simplex, shared by multiple elements, have a globally unique index. Given the one-to-one relationship between interpolation points and DoFs, this is equivalent to providing an indexing rule for global DoFs in the scalar Lagrange finite element space. Based on this, we will further discuss the indexing rules for DoFs in face and edge finite element spaces.

## 6.1 Lagrange finite element space

We begin by discussing the data structure of the tetrahedral mesh, denoted by  $\mathcal{T}_h$ . Let the numbers of nodes, edges, faces, and cells in  $\mathcal{T}_h$  be represented as NN, NE, NF, and NC, respectively. We utilize two arrays to represent  $\mathcal{T}_h$ :

- `node` (shape: (NN, 3)): `node[i, j]` represents the  $j$ -th component of the Cartesian coordinate of the  $i$ -th vertex.
- `cell` (shape: (NC, 4)): `cell[i, j]` gives the global index of the  $j$ -th vertex of the  $i$ -th cell.

Given a tetrahedron denoted by  $[0, 1, 2, 3]$ , we define its local edges and faces as:

- `SEdge` =  $[(0, 1), (0, 2), (0, 3), (1, 2), (1, 3), (2, 3)]$ ;
- `SFace` =  $[(1, 2, 3), (0, 2, 3), (0, 1, 3), (0, 1, 2)]$ ;
- `OFace` =  $[(1, 2, 3), (0, 3, 2), (0, 1, 3), (0, 2, 1)]$ ;

Here, we introduced two types of local faces. The prefix S implies sorting, and O indicates outer normal direction. Both `SFace[i, :]` and `OFace[i, :]` represent the face opposite to the  $i$ -th vertex but with varied ordering. The normal direction as determined by the ordering of the three vertices of `OFace` matches the outer normal direction of the tetrahedron. This ensures that the outer normal direction of a boundary face points outward from the mesh. Meanwhile, `SFace` aids in determining the global index of the interpolation points on the face. For an in-depth discourse on indexing, ordering, and orientation, we direct readers to `sc3` in *iFEM* [15].

Leveraging the unique algorithm for arrays, we can derive the following arrays from `cell`, `SEdge`, and `OFace`:

- `edge` (shape: (NE, 2)): `edge[i, j]` gives the global index of the  $j$ -th vertex of the  $i$ -th edge.
- `face` (shape: (NF, 3)): `face[i, j]` provides the global index of the  $j$ -th vertex of the  $i$ -th face.
- `cell2edge` (shape: (NC, 6)): `cell2edge[i, j]` indicates the global index of the  $j$ -th edge of the  $i$ -th cell.
- `cell2face` (shape: (NC, 4)): `cell2face[i, j]` signifies the global index of the  $j$ -th face of the  $i$ -th cell.

Having constructed the edge and face arrays and linked cells to them, we next establish indexing rules for interpolation points on  $\mathcal{T}_h$ . Let  $k$  be the degree of the Lagrange finite element space. The number of interpolation points on each cell is

$$\text{ldof} = \dim \mathbb{P}_k(T) = \frac{(k+1)(k+2)(k+3)}{6},$$

and the total number of interpolation points on  $\mathcal{T}_h$  is

$$\text{g dof} = \text{NN} + n_e^k \cdot \text{NE} + n_f^k \cdot \text{NF} + n_c^k \cdot \text{NC},$$

where

$$n_e^k = k-1, \quad n_f^k = \frac{(k-2)(k-1)}{2}, \quad n_c^k = \frac{(k-3)(k-2)(k-1)}{6},$$

are numbers of interpolation points inside edge, face, and cell, respectively. We need an index mapping from  $[0:\text{ldof}-1]$  to  $[0:\text{g dof}-1]$ . See Fig. 4 for an illustration of the local index and the global index of interpolation points.

The tetrahedron's four vertices are ordered according to the right-hand rule, and the interpolation points adhere to the dictionary ordering map  $R_3(\alpha)$ . As Lagrange element is globally continuous, the indexing of interpolation points on the boundary  $\partial T$  should be global. Namely a unique index for points on vertices, edges, faces should be used and a mapping from the local index to the global index is needed.

We first set a global indexing rule for all interpolation points. We sort the index by vertices, edges, faces, and cells. For the interpolation points that coincide with the vertices, their global index are set as  $0, 1, \dots, \text{NN}-1$ . When  $k > 1$ , for the interpolation points that inside edges, their global index are set as

$$\begin{matrix} 0 \\ 1 \\ \vdots \\ \text{NE}-1 \end{matrix} \begin{pmatrix} 0 \cdot n_e^k & \cdots & 1 \cdot n_e^k - 1 \\ 1 \cdot n_e^k & \cdots & 2 \cdot n_e^k - 1 \\ \vdots & & \vdots \\ (\text{NE}-1) \cdot n_e^k & \cdots & \text{NE} \cdot n_e^k - 1 \end{pmatrix} + \text{NN}.$$

Here recall that  $n_e^k = k-1$  is the number of interior interpolation points on an edge. When  $k > 2$ , for the interpolation points that inside each face, their global index are set as

$$\begin{matrix} 0 \\ 1 \\ \vdots \\ \text{NF}-1 \end{matrix} \begin{pmatrix} 0 \cdot n_f^k & \cdots & 1 \cdot n_f^k - 1 \\ 1 \cdot n_f^k & \cdots & 2 \cdot n_f^k - 1 \\ \vdots & & \vdots \\ (\text{NF}-1) \cdot n_f^k & \cdots & \text{NF} \cdot n_f^k - 1 \end{pmatrix} + \text{NN} + \text{NE} \cdot n_e^k,$$

where  $n_f^k = (k-2)(k-1)/2$  is the number of interior interpolation points on  $f$ . When  $k > 3$ , the global index of the interpolation points that inside each cell can be set in a similar way.

Then we use the two-dimensional array named `cell2ipoint` of shape  $(\text{NC}, \text{ldof})$  for the index map. On the  $j$ -th interpolation point of the  $i$ -th cell, we aim to determine its unique global index and store it in `cell2ipoint[i, j]`.

For vertices and cell interpolation points, the mapping is straightforward by the global indexing rule. Indeed `cell` is the mapping of the local index of a vertex to its global index. However, complications arise when the interpolation point is located within an edge or face due to non-unique representations of an edge and a face.

We use the more complicated face interpolation points as a typical example to illustrate the situation. Consider, for instance, the scenario where the  $j$ -th interpolation point lies within the 0-th

local face  $F_0$  of the  $i$ -th cell. Let  $\alpha = \mathbf{m} = [m_0, m_1, m_2, m_3]$  be its lattice point. Given that  $F_0$  is opposite to vertex 0, we deduce that  $\lambda_0|_{F_0} = 0$ , which implies  $m_0$  is 0. The remaining components of  $\mathbf{m}$  are non-zero, ensuring that the point is interior to  $F_0$ .

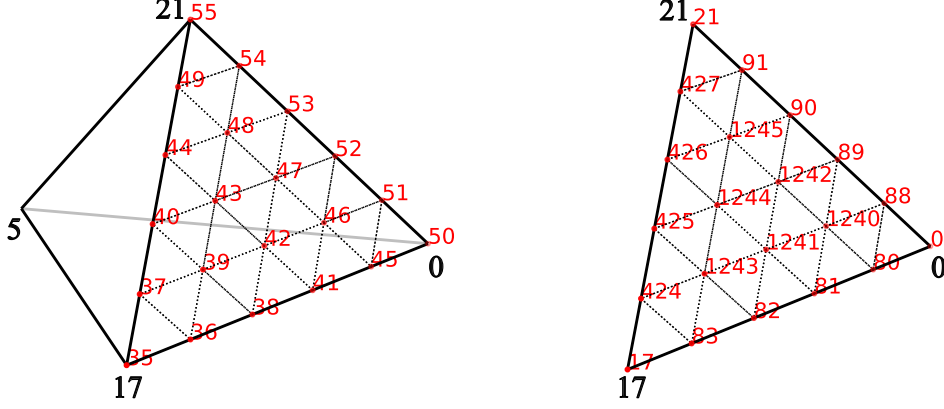


Figure 4: Local indexing (Left) and global indexing (Right) of DoFs for a face of tetrahedron, where the local vertex order is  $[17, 0, 21]$  and global vertex order is  $[0, 17, 21]$ . Due to the different ordering of vertices in local and global representation of the face, the ordering of the local indexing and the global indexing is different.

Two representations for the face with global index  $\text{cell2face}[i, 0]$  are subsequently acquired:

- $\text{LFace} = \text{cell}[i, \text{SFace}[0, :]]$  (local representation)
- $\text{GFace} = \text{face}[\text{cell2face}[i, 0], :]$  (global representation)

Although  $\text{LFace}$  and  $\text{GFace}$  comprise identical vertex numbers, their ordering differs. For example,  $\text{LFace} = [5 \ 6 \ 10]$  while  $\text{GFace} = [10 \ 6 \ 5]$ .

The array  $\mathbf{m} = [m_1, m_2, m_3]$  has a one-to-one correspondence with the vertices of  $\text{LFace}$ . To match this array with the vertices of  $\text{GFace}$ , a reordering based on argument sorting is performed:

```

1 i0 = argsort(argsort(GFace));
2 i1 = argsort(LFace);
3 i2 = i1[i0];
4 m = m[i2];

```

In the example of  $\text{LFace} = [5 \ 6 \ 10]$  while  $\text{GFace} = [10 \ 6 \ 5]$ , the input  $\mathbf{m} = [m_1, m_2, m_3]$  will be reordered to  $\mathbf{m} = [m_3, m_2, m_1]$ .

From the reordered  $\mathbf{m} = [m_1, m_2, m_3]$ , the local index  $\ell$  of the  $j$ -th interpolation point on

the global face  $f = \text{cell2face}[i, 0]$  can be deduced:

$$\begin{aligned}\ell &= \frac{(m_2 - 1 + m_3 - 1)(m_2 - 1 + m_3 - 1 + 1)}{2} + m_3 - 1 \\ &= \frac{(m_2 + m_3 - 2)(m_2 + m_3 - 1)}{2} + m_3 - 1.\end{aligned}$$

It's worth noting that the index of interpolation points solely within the face needs consideration. Finally, the global index for the  $j$ -th interpolation point within the 0-th local face of the  $i$ -th cell is:

$$\text{cell2ipoint}[i, j] = \text{NN} + n_e^k \cdot \text{NE} + n_f^k \cdot f + \ell.$$

Here, we provide a specific example. Consider a 5th-degree Lagrange finite element space on the  $c$ -th tetrahedron in a mesh depicted in Fig. 4. The vertices of this tetrahedron are  $[5, 17, 0, 21]$ , and its 0th face is denoted as  $f$ , with vertices  $[0, 17, 21]$ . Assuming that

$$\text{NN} + n_e^k \cdot \text{NE} + n_f^k \cdot f = 1240.$$

For the 39-th local DoF on tetrahedron, its corresponding multi-index is  $[0, 3, 1, 1]$  on cell and  $[3, 1, 1]$  on face. Since the local face is  $[17, 0, 21]$  and the global face is  $[0, 17, 21]$ , then  $m = [1, 3, 1]$  and  $\ell = 3$  thus

$$\text{cell2ipoint}[c, 39] = 1243.$$

Similar, for the 43-th local DoF on tetrahedron,  $m = [1, 2, 2]$  and  $\ell = 4$  thus

$$\text{cell2ipoint}[c, 43] = 1244.$$

Fig. 4 shows the correspondence between the local and the global indexing of DoFs for the cell.

In conclusion, we've elucidated the construction of global indexing for interpolation points inside cell faces. This method can be generalized for edges and, more broadly, for interior interpolation points of the low-dimensional sub-simplex of an  $n$ -dimensional simplex. Please note that for scalar Lagrange finite element spaces, the `cell2ipoint` array is the mapping array from local DoFs to global DoFs.

## 6.2 Face and edge finite element spaces

First, we want to emphasize that the management of DoFs is to manage the continuity of finite element space.

The BDM and second-kind Nédélec are vector finite element spaces, which define DoFs of vector type by defining a vector frame on each interpolation point. At the same time, they define their vector basis functions by combining the Lagrange basis function and the dual frame of the DoFs.

Alternatively, we can say each DoF in BDM or second-kind Nédélec space corresponds to a unique interpolation point  $p$  and a unique vector  $e$ , and each basis function also corresponds to a unique Lagrange basis function which is defined on  $p$  and a vector  $\hat{e}$  which is the dual to  $e$ .



The management of DoFs is essentially a counting problem. First of all, we need to set global and local indexing rules for all DoFs. We can globally divide the DoFs into shared and unshared among simplexes. The DoFs shared among simplexes can be further divided into on-edge and on-face according to the dimension of the sub-simplex where the DoFs locate. First count the shared DoFs on each edge according to the order of the edges, then count the shared DoFs on each face according to the order of the faces, and finally count the unshared DoFs in the cell. On each edge or face, the DoFs' order can follow the order of the interpolation points. Note that, for BDM and second-kind Nédélec space there are no DoFs shared on nodes. And for 3D BDM space there are no DoFs shared on edges. So the global numbering rule is similar with the Lagrange interpolation points.

According to the global indexing rule, we also can get a array named `dof2vector` with shape  $(\text{gdof}, \text{GD})$ , where `gdof` is the number of global DoFs and `GD` represent geometry dimensions. And `dof2vector[i, :]` store the vector of the  $i$ -th DoF.

Next we need to set a local indexing rules and generate a array `cell2dof` with shape  $(\text{NC}, \text{ldof})$ , where `ldof` is the number of local DoFs on each cell. Note that each DoF was determined by an interpolation point and a vector. And for each interpolation point, there is a frame (including `GD` vectors) on it. Given a DoF on  $i$ -th cell, denote the local index of its interpolation point as  $p$ , and the local index of its vector in the frame denote as  $q$ , then one can set a unique local index number  $j$  by  $p$  and  $q$ , for example  $j = n \cdot q + p$ , where  $n$  is the number of interpolation points in  $i$ -th cell. Furthermore, we can compute the `cell2dof[i, j]` by the global index `cell2ipoint[i, p]`, the sub-simplex that the interpolation point locate, and the global indexing rule.

**Remark 6.1.** Note that the local and global number rules mentioned above are not unique. Furthermore, with the array `cell2dof`, the implementation of these higher-order finite element methods mentioned in this paper is not fundamentally different from the conventional finite element in terms of matrix vector assembly and boundary condition handling.  $\square$

## 7 Numerical Examples

In this section, we numerically verify the 3-dimensional BDM elements basis and the second kind of Nédélec element basis using two test problems over the domain  $\Omega = (0,1)^3$  partitioned into a structured tetrahedron mesh  $\mathcal{T}_h$ . All the algorithms and numerical examples are implemented based on the FEALPy package [33].

### 7.1 High Order Elements for Poisson Equation in the Mixed Formulation

Consider the Poisson problem:

$$\begin{cases} \mathbf{u} + \nabla p = 0 & \text{in } \Omega, \\ \nabla \cdot \mathbf{u} = f & \text{in } \Omega, \\ p = g & \text{on } \partial\Omega. \end{cases}$$

The variational problem is : find  $\mathbf{u} \in H(\text{div}, \Omega)$ ,  $p \in L^2(\Omega)$ , satisfy:

$$\begin{aligned} \int_{\Omega} \mathbf{u} \cdot \mathbf{v} \, dx - \int_{\Omega} p \nabla \cdot \mathbf{v} \, dx &= - \int_{\partial\Omega} g(\mathbf{v} \cdot \mathbf{n}) \, ds, \quad \mathbf{v} \in H(\text{div}, \Omega), \\ - \int_{\Omega} (\nabla \cdot \mathbf{u}) q \, dx &= - \int_{\Omega} f q \, dx, \quad q \in L^2(\Omega). \end{aligned}$$

Let  $V_{h,k}^{\text{div}}$  be the BDM space with degree  $k$  on  $\mathcal{T}_h$  and piecewise polynomial space of degree  $k-1$  on  $\mathcal{T}_h$  by  $V_{k-1}$ . The corresponding finite element method is: find  $\mathbf{u}_h \in V_{h,k}^{\text{div}}$ ,  $p_h \in V_{k-1}$ , such that

$$\int_{\Omega} \mathbf{u}_h \cdot \mathbf{v}_h \, dx - \int_{\Omega} p_h \nabla \cdot \mathbf{v}_h \, dx = - \int_{\partial\Omega} g(\mathbf{v}_h \cdot \mathbf{n}) \, ds \quad \mathbf{v}_h \in V_{h,k}^{\text{div}}, \quad (7.1)$$

$$- \int_{\Omega} (\nabla \cdot \mathbf{u}_h) q_h \, dx = - \int_{\Omega} f q_h \, dx, \quad q_h \in V_{k-1}. \quad (7.2)$$

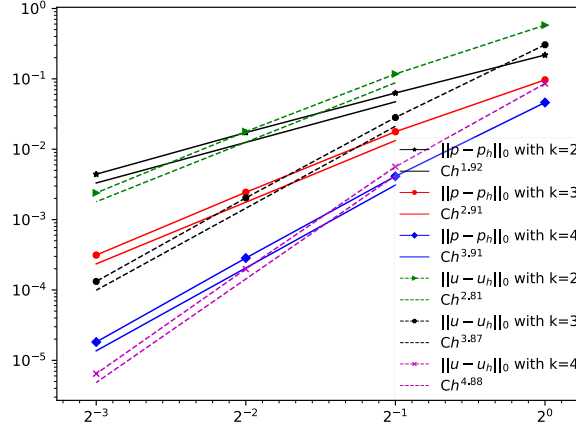


Figure 5: Errors  $\|\mathbf{u} - \mathbf{u}_h\|_0$  and  $\|p - p_h\|_0$  of finite element method (7.1) and (7.2) on uniformly refined mesh with  $k=2,3,4$ .

To test the convergence order of BDM space, we set

$$\mathbf{u} = \begin{pmatrix} -\pi \sin(\pi x) \cos(\pi y) \cos(\pi z) \\ -\pi \cos(\pi x) \sin(\pi y) \cos(\pi z) \\ -\pi \cos(\pi x) \cos(\pi y) \sin(\pi z) \end{pmatrix},$$

$$p = \cos(\pi x) \cos(\pi y) \cos(\pi z), \quad f = 3\pi^2 \cos(\pi x) \cos(\pi y) \cos(\pi z).$$

The numerical results are shown in Fig. 5 and it is clear that

$$\|\mathbf{u} - \mathbf{u}_h\|_0 \leq Ch^{k+1}, \quad \|p - p_h\|_0 \leq Ch^k.$$

## 7.2 High Order Elements for Maxwell Equations

Consider the time harmonic problem:

$$\begin{cases} \nabla \times (\mu^{-1} \nabla \times E) - \omega^2 \tilde{\epsilon} E = J & \text{in } \Omega, \\ n \times E = 0 & \text{on } \partial\Omega. \end{cases}$$

The variational problem is: find  $E \in H_0(\text{curl}, \Omega)$ , satisfies:

$$\int_{\Omega} \mu^{-1} (\nabla \times E) \cdot (\nabla \times v) \, dx - \int_{\Omega} \omega^2 \tilde{\epsilon} E \cdot v \, dx = \int_{\Omega} J \cdot v \, dx \quad \forall v \in H_0(\text{curl}, \Omega).$$

Let  $\mathring{V}_{h,k}^{\text{curl}} = V_{h,k}^{\text{curl}} \cap H_0(\text{curl}, \Omega)$ , where  $V_{h,k}^{\text{curl}}$  is the edge element space defined in Theorem ??.

The corresponding finite element method is: find  $E_h \in \mathring{V}_{h,k}^{\text{curl}}$  s.t.

$$\int_{\Omega} \mu^{-1} (\nabla \times E_h) \cdot (\nabla \times v_h) \, dx - \int_{\Omega} \omega^2 \tilde{\epsilon} E_h \cdot v_h \, dx = \int_{\Omega} J \cdot v_h \, dx, \quad v_h \in \mathring{V}_{h,k}^{\text{curl}}. \quad (7.3)$$

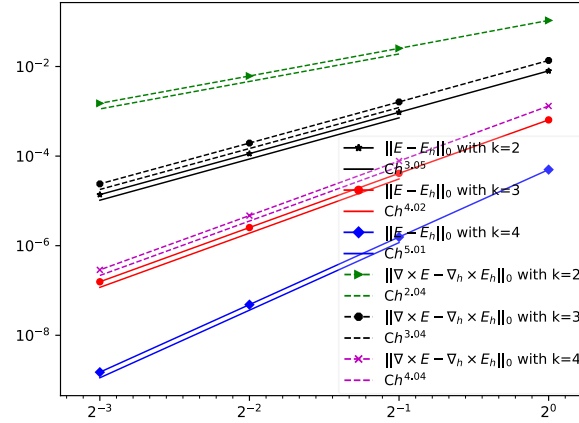


Figure 6: Errors  $\|E - E_h\|_0$  and  $\|\nabla \times (E - E_h)\|_0$  of finite element method (7.3) on uniformly refined mesh with  $k=2,3,4$ .

To test the convergence rate of second-kind Nédélec space, we choose

$$\begin{aligned} \omega &= \tilde{\epsilon} = \mu = 1, & E &= (f, \sin(x)f, \sin(y)f), \\ f &= (x^2 - x)(y^2 - y)(z^2 - z), & J &= \nabla \times \nabla \times E - E. \end{aligned}$$

The numerical results are shown in Fig. 6 and it is clear that

$$\|E - E_h\|_0 \leq Ch^{k+1}, \quad \|\nabla \times (E - E_h)\|_0 \leq Ch^k.$$

## Acknowledgments

The first and fourth authors were supported by the National Natural Science Foundation of China (NSFC) (Grant No. 12371410, 12261131501), and the construction of innovative provinces in Hunan Province (Grant No. 2021GK1010). The second author was supported by NSF DMS-2012465 and DMS-2309785. The third author was supported by the National Natural Science Foundation of China (NSFC) (Grant No. 12171300), and the Natural Science Foundation of Shanghai (Grant No. 21ZR1480500).

## References

- [1] M. Ainsworth, G. Andriamaro, and O. Davydov. A Bernstein–Bézier basis for arbitrary order Raviart–Thomas finite elements. *Constr. Approx.*, 41:1–22, 2015.
- [2] M. Ainsworth and J. Coyle. Hierarchic finite element bases on unstructured tetrahedral meshes. *Internat. J. Numer. Methods Engrg.*, 58(14):2103–2130, 2003.
- [3] M. Ainsworth and G. Fu. Bernstein–Bézier bases for tetrahedral finite elements. *Comput. Methods Appl. Mech. Engrg.*, 340:178–201, 2018.
- [4] M. Alnæs, J. Blechta, J. Hake, A. Johansson, B. Kehlet, A. Logg, C. Richardson, J. Ring, M. E. Rognes, and G. N. Wells. The fenics project version 1.5. *Archive of numerical software*, 3(100), 2015. [3](#)
- [5] R. Anderson, J. Andrej, A. Barker, J. Bramwell, J.-S. Camier, J. Cervený, V. Dobrev, Y. Dudouit, A. Fisher, T. Kolev, et al. Mfem: A modular finite element methods library. *Comput. Math. Appl.*, 81:42–74, 2021.
- [6] E. Andreassen, A. Clausen, M. Schevenels, B. S. Lazarov, and O. Sigmund. Efficient topology optimization in matlab using 88 lines of code. *Structural and Multidisciplinary Optimization*, 43:1–16, 2011. [3](#)
- [7] D. N. Arnold, R. S. Falk, and R. Winther. Finite element exterior calculus, homological techniques, and applications. *Acta Numer.*, 15:1–155, 2006. [15](#), [17](#), [18](#)
- [8] D. N. Arnold, R. S. Falk, and R. Winther. Geometric decompositions and local bases for spaces of finite element differential forms. *Comput. Methods Appl. Mech. Engrg.*, 198(21-26):1660–1672, May 2009. [6](#), [7](#)
- [9] M. P. Bendsøe and O. Sigmund. *Topology optimization by distribution of isotropic material*, pages 1–69. Springer Berlin Heidelberg, Berlin, Heidelberg, 2004. [3](#)
- [10] J. Bradbury, R. Frostig, P. Hawkins, M. J. Johnson, C. Leary, D. Maclaurin, G. Necula, A. Paszke, J. VanderPlas, S. Wanderman-Milne, et al. Jax: composable transformations of python+ numpy programs. 2018. [4](#)
- [11] F. Brezzi, J. Douglas, Jr., R. Durán, and M. Fortin. Mixed finite elements for second order elliptic problems in three variables. *Numer. Math.*, 51(2):237–250, 1987.
- [12] F. Brezzi, J. Douglas, Jr., and L. D. Marini. Two families of mixed finite elements for second order elliptic problems. *Numer. Math.*, 47(2):217–235, 1985.
- [13] D. A. Castro, P. R. B. Devloo, A. M. Farias, S. M. Gomes, D. de Siqueira, and O. Durán. Three dimensional hierarchical mixed finite element approximations with enhanced primal variable accuracy. *Comput. Methods Appl. Mech. Engrg.*, 306:479–502, 2016. [13](#)
- [14] A. Chandrasekhar, S. Sridhara, and K. Suresh. Auto: a framework for automatic differentiation in topology optimization. *Structural and Multidisciplinary Optimization*, 64(6):4355–4365, 2021. [4](#)

- [15] L. Chen. iFEM: an innovative finite element methods package in MATLAB. *In Preparation*, 2008. 21
- [16] L. Chen and X. Huang. Geometric decomposition of div-conforming finite element tensors. *arXiv preprint arXiv:2112.14351v1*, 2021. 7, 11
- [17] L. Chen and X. Huang. Finite element de Rham and Stokes complexes in three dimensions. *Math. Comp.*, 93(345):55–110, 2024. 6
- [18] S. H. Christiansen, J. Hu, and K. Hu. Nodal finite element de Rham complexes. *Numer. Math.*, 139(2):411–446, 2018.
- [19] H. Chung, J. T. Hwang, J. S. Gray, and H. A. Kim. Topology optimization in openmdao. *Structural and multidisciplinary optimization*, 59:1385–1400, 2019. 3
- [20] D. De Siqueira, P. R. B. Devloo, and S. M. Gomes. Hierarchical high order finite element approximation spaces for  $H(\text{div})$  and  $H(\text{curl})$ . In G. Kreiss, P. Lötstedt, A. Målqvist, and M. Neytcheva, editors, *Numerical Mathematics and Advanced Applications 2009*, pages 269–276, Berlin, Heidelberg, 2010. Springer Berlin Heidelberg. 13
- [21] D. De Siqueira, P. R. B. Devloo, and S. M. Gomes. A new procedure for the construction of hierarchical high order  $H\text{div}$  and  $H\text{curl}$  finite element spaces. *J. Comput. Appl. Math.*, 240:204–214, 2013. 13
- [22] V. Ervin. Computational bases for  $RT_k$  and  $BDM_k$  on triangles. *Comput. Math. Appl.*, 64(8):2765–2774, 2012.
- [23] R. M. Ferro and R. Pavanello. A simple and efficient structural topology optimization implementation using open-source software for all steps of the algorithm: Modeling, sensitivity analysis and optimization. *CMES-Computer Modeling in Engineering & Sciences*, 136(2), 2023. 3
- [24] J. S. Gray, J. T. Hwang, J. R. Martins, K. T. Moore, and B. A. Naylor. Openmdao: An open-source framework for multidisciplinary design, analysis, and optimization. *Structural and Multidisciplinary Optimization*, 59(4):1075–1104, 2019. 3
- [25] A. Griewank and A. Walther. *Evaluating derivatives: principles and techniques of algorithmic differentiation*. SIAM, 2008. 3
- [26] A. Gupta, R. Chowdhury, A. Chakrabarti, and T. Rabczuk. A 55-line code for large-scale parallel topology optimization in 2d and 3d. *arXiv preprint arXiv:2012.08208*, 2020. 3
- [27] K. Liu and A. Tovar. An efficient 3d topology optimization code written in matlab. *Structural and multidisciplinary optimization*, 50(6):1175–1196, 2014. 3
- [28] J.-C. Nédélec. A new family of mixed finite elements in  $\mathbf{R}^3$ . *Numer. Math.*, 50(1):57–81, 1986. 17
- [29] R. Nicolaides. On a class of finite elements generated by lagrange interpolation. *SIAM J. Numer. Anal.*, 9(3):435–445, 1972. 5, 9
- [30] S. A. Nørgaard, M. Sagebaum, N. R. Gauger, and B. S. Lazarov. Applications of automatic differentiation in topology optimization. *Structural and Multidisciplinary Optimization*, 56:1135–1146, 2017. 4
- [31] M. E. Rognes, R. C. Kirby, and A. Logg. Efficient assembly of  $H(\text{div})$  and  $H(\text{curl})$  conforming finite elements. *SIAM J. Sci. Comput.*, 31(6):4130–4151, 2010.
- [32] O. Sigmund. A 99 line topology optimization code written in matlab. *Structural and multidisciplinary optimization*, 21(2):120–127, 2001. 3
- [33] H. Wei, C. Chen, and Y. Huang. FEALPy: Finite Element Analysis Library in Python. <https://github.com/weihuayi/fealpy>, Xiangtan University, 2017-2024. 25
- [34] J. Xin and W. Cai. A well-conditioned hierarchical basis for triangular  $H(\text{curl})$ -conforming elements. *Commun. Comput. Phys.*, 9(3):780–806, 2011.
- [35] J. Xin, W. Cai, and N. Guo. On the construction of well-conditioned hierarchical bases for (div)-conforming  $\mathbb{R}^n$  simplicial elements. *Commun. Comput. Phys.*, 14(3):621–638, 2013.

- [36] J. Xin, N. Guo, and W. Cai. On the construction of well-conditioned hierarchical bases for tetrahedral  $H(\text{curl})$ -conforming Nédélec element. *J. Comput. Math.*, pages 526–542, 2011.